Electron-loss calculations using the free-collision model

Mati Meron and Brant M. Johnson
Department of Applied Science, Brookhaven National Laboratory, Upton, New York 11973
(Received 20 September 1989)

There have been very few measurements of electron-loss cross sections for high-energy (> 1 MeV) negative and neutral hydrogen projectiles interacting with gas targets. Previous approaches to the estimation of these cross sections have been based mainly on semiempirical fits aimed at tying the existing low-energy data to theoretical high-energy Born approximation values. Such target-dependent approaches are reliable only for targets for which a sufficient amount of experimental data exists. The more general approach presented here is based on the free-collision model and uses global properties of the momentum-domain atomic form factor to calculate electron-loss cross sections. The results are simple functions of E and Z, with a small number of target-independent parameters. For each single-electron-loss cross section, $\sigma_{-1,0}$ and $\sigma_{0,1}$, fits to available data are presented.

I. INTRODUCTION

The calculation of electron-loss cross sections in atomic collisions is a long-standing problem in atomic physics, with important fundamental ramifications and far-reaching practical applications. In spite of considerable effort over the past few decades, the single-electron-loss problem is understood only in the high-velocity limit. Even for the simplest processes of this kind, such as single-electron stripping from H^0 and H^- interacting with a noble-gas target, there is no exact theory — or even an approximation — capable of predicting electron-loss cross sections over a broad energy range and for all possible targets.

At very high collision velocities, accurate results for the electron-loss cross sections can be obtained using the Born approximation[1-3] (BA) and its variations. These results and the associated concept of asymptotic collision strength are applicable only for $v_p \gg v_e$, where v_p is the projectile velocity and v_e is the equivalent bound electron velocity. At the opposite limit of $v_p \ll v_e$, the collision is best described in terms of creation and dissociation of molecular orbitals (MO), and an individual treatment is needed for each target-projectile combination. Between these two extremes there is a broad velocity regime, commonly referred to as $v_p \approx v_e$, but actually extending way above and below the $v_p = v_e$ point, in which both the BA and the MO approaches are not applicable.

While most of the existing experimental electron-loss data lie in the region of $v_p \approx v_e$, theoretically this velocity regime remains largely *terra incognita*. The few theoretical advances that have been made are mostly limited to studies of specific cases in the vicinity of $v_p = v_e$. There has been some previous work for velocities between $v_p \approx v_e$ and the high-velocity limit but the effort is mostly focused on empirical fits to the scanty experimental data. While being of some usefulness, especially when designed to converge to the BA results at the high-velocity limit, these target-dependent fits are powerless when it comes to estimating the stripping cross sections for targets for which no data exist. What is obviously missing is a general approach for calculating cross sections in the intermediate velocity regime for a broad range of targets.

Apart from the obvious desire to further a basic understanding of fundamental ion-atom collision processes, an additional motivation for this work is the goal of providing an accurate atomic data base for applied research. For example, cross sections for negative-ion neutralization in a gas neutralizer are of interest in various schemes for neutral-beam heating of fusion devices. An exact theory would be most desirable, but a useful temporary substitute would be a semiempirical model capable of generating electron-stripping cross sections (e.g., for H^- and H^0) with reasonable accuracy over a broad range of energies and target atomic numbers. That is the goal of this work.

A model based on the free-collision approximation is described herein. This approach achieves the above-stated goal without being unduly complicated. First, the basic model and several alternative formulations are discussed. Next, calculations based on each formulation are described. Then, for each case a small number of adjustable parameters are fixed by fitting to existing data on various targets. Finally, a recipe for the estimation of electron-loss cross sections is presented. As the approach used here is quite general, it is reasonable to expect that it can be applied also to more complex collision systems.

II. THE FREE-COLLISION MODEL

The free-collision model[4] (FCM) has been used extensively in the past to estimate ionization cross sections.

It is based on the assumption that the ionization of the projectile can be regarded as Rutherford scattering of a projectile's electron by the screened Coulomb potential of the target atom. In other words the electron traveling with the projectile nucleus is considered as essentially free as long as the energy provided by the scattering process exceeds the binding energy.

Using atomic units, the differential scattering cross section written as a function of the momentum transfer is given by

$$\frac{d\sigma}{dq} = \frac{8\pi}{v^2}\frac{[Z - F(q)]^2}{q^3}, \tag{2.1}$$

where Z is the target atomic number, v is the collision velocity, and $F(q)$ is the atomic form factor of the target atom. The momentum transfer q is given by

$$q = 2v \sin\frac{\theta}{2}, \tag{2.2}$$

where θ is the scattering angle. To obtain the total ionization cross section the expression in Eq. (2.1) is integrated over the momentum range from $q_{\min}$ to $q_{\max}$, where $q_{\min} = v_i$, which is the velocity corresponding to the ionization energy, and $q_{\max} = 2v$, which follows from kinematic considerations.

At high energies the FCM results converge to those of the BA, from which they are derived. As the energy is decreased, the calculated results will gradually diverge from the physical cross sections due to the violation of the free-collision assumption. However, this tendency to diverge can be easily overcome by introducing semiempirical corrections. The minimal velocity v_i introduced above is a simple example of such a correction, and a more general approach will be presented in the next section. While in principle similar corrections can be introduced in the BA, the results are considerably more complex.

At the time of its introduction, the FCM was hampered by the complexity of atomic form factor calculations. The situation is now improved, and numerical calculations of $F(q)$ have been carried out for many atoms.[5-10] Still, the fact remains that even if the best available $F(q)$ results are used the FCM cross sections can only be calculated numerically, never in a closed analytical form. As such they are not easy to use in practical applications, where quite often knowledge of the cross section's behavior over a wide range of energy and/or possible targets is more valuable than precision. That explains why the FCM approach was not widely used in the past.

III. FORMALISM DEVELOPMENT

As noted above, the complexity of the FCM approach is caused by the need to separately calculate the atomic form factor for each target and for each momentum transfer. However, examination of the existing data for the H^0 and H^- electron-loss cross sections shows that the functional dependence on energy is remarkably smooth and roughly similar for all targets. This seems to indicate that it is mainly the general behavior of the form factors that determines the cross sections, and that target-structure-dependent differences in the $F(q)$ are relatively unimportant (except, possibly, at extremely low velocities). Therefore, if a reasonably simple function of q and Z can be found that reproduces the general functional form of the $F(q)$'s, then the cross section calculations can be greatly simplified without sacrificing accuracy.

As the first step toward achieving this goal, the cross section expression in Eq.(2.1) can be rewritten in the form

$$\frac{d\sigma}{dq} = \frac{8\pi Z^2}{v^2}\frac{[1 - f(q)]^2}{q^3}, \tag{3.1}$$

where $f(q)$ is the normalized form factor expressed in terms of the radial electron density $\rho(r)$ as

$$f(q) = \int_0^\infty r\rho(r)\frac{\sin qr}{q}dr, \tag{3.2}$$

and where $\rho(r)$ fulfills

$$\int_0^\infty r^2\rho(r)dr = 1. \tag{3.3}$$

Both Eq. (3.2) and Eq. (3.3) are based on the assumption that the electron density is spherically symmetric. While strictly true only for closed-shell atoms, this assumption is nevertheless justified by the fact that in single-collision measurements the target atoms are usually randomly oriented. Therefore, unless a special effort is made to polarize the target, the measured cross sections are an average over all possible target orientations.

Now, based on the previous discussion, the total loss cross section is given by

$$\sigma = \frac{8\pi Z^2}{v^2}\int_{v_i}^{2v}\frac{[1 - f(q)]^2}{q^3}dq. \tag{3.4}$$

However, this expression implies a sharp cutoff at v_i, contrary to the behavior of the experimental data. Therefore it is preferable to use the more general expression

$$\sigma = \frac{8\pi Z^2}{v^2}\int_0^{2v}\frac{[1 - f(q)]^2 P(q, v_i)}{q^3}dq, \tag{3.5}$$

where $P(q, v_i)$ is an ionization probability, yet to be determined.

Equation (3.5) can be significantly simplified using the assumption that the electron density can be represented by

$$\rho(r) = \frac{1}{R^3}\tilde{\rho}\left(\frac{r}{R}\right), \tag{3.6}$$

where $\tilde{\rho}$ is a universal function and R is a Z-dependent scaling radius. A typical example of this type of electron density is the well-known Thomas-Fermi distribution. While admittedly less sophisticated and precise than modern $\rho(r)$ results, distributions of this form have the advantage of easily yielding the target Z dependence of the process under study, albeit with some loss of accuracy.

The substitution of Eq. (3.6) into Eq. (3.2) yields

$$f(q) = \int_0^\infty \frac{r\,dr}{R^2}\frac{1}{R^3}\tilde{\rho}\left(\frac{r}{R}\right)\frac{\sin[qR(r/R)]}{qR}R^3$$
$$= \int_0^\infty t\tilde{\rho}(t)\frac{\sin st}{s}dt$$
$$= \tilde{f}(s), \tag{3.7}$$

where $s = qR$, and $\tilde{f}(s)$ is also a universal function. Now, using Eq. (3.7) in Eq. (3.5) the cross section can be rewritten in the form

$$\sigma = \frac{8\pi Z^2}{v^2}\int_0^{2v}\frac{[1-\tilde{f}(s)]^2 P(s/R, v_i)}{(s/R)^3}d(s/R)$$
$$= \frac{8\pi Z^2 R^2}{v^2}\int_0^{2vR}\frac{[1-\tilde{f}(s)]^2\tilde{P}(s, v_i R)}{s^3}ds. \tag{3.8}$$

In this last form the whole target dependence (except for the Z^2 multiplier) is contained in the parameter R.

In Appendix A it is shown that Eq. (3.7) can be used to deduce the asymptotic behavior of the function $\tilde{f}(s)$, in the limit of small and large values of s. It is also shown there, using the fact that the scaling radius R (and therefore also s) is determined only to within a multiplicative constant, that the simplest possible choices for a function $\tilde{f}(s)$ satisfying these asymptotic conditions are

$$\tilde{f}_s(s) = \frac{1}{s^2+1} \tag{3.9}$$

for a density function with a singularity at the origin, and

$$\tilde{f}_r(s) = \frac{1}{(s^2+\gamma)(s^2+\gamma^{-1})}, \tag{3.10}$$

where γ is an arbitrary positive constant, for a regular $\tilde{\rho}$. Both forms of $\tilde{f}(s)$ will be used in the subsequent calculations. It could be argued at this point that since electron densities are well known to be regular, the singular form should not be considered. It turns out, however, that the singularity assumption has a negligible effect on the total-cross-section results, while (as will be shown in the next section) greatly simplifying the resultant expressions. This point will be elaborated further in Sec. V.

Before the integral in Eq. (3.8) can be evaluated, a simple representation of the ionization probability $\tilde{P}(s, v_i R)$ is needed. In general, $\tilde{P}(s, v_i R) \to 0$ as $s \to 0$ and $\tilde{P}(s, v_i R)$ is expected to asymptotically approach unity (or at least a constant) as s goes to infinity. Since, given the assumption of a rotationally invariant $\rho(r)$, the ionization probability cannot depend on the direction of the momentum transfer, $\tilde{P}(s, v_i R)$ should be an even function of s. Two simple guesses for $\tilde{P}$ are either a sharp cutoff, i.e.,

$$\tilde{P}_1(s, v_i R) = \begin{cases} 0 & \text{for } s < v_i R \\ 1 & \text{for } s \geq v_i R, \end{cases} \tag{3.11}$$

or a gradual transition from no ionization to full ionization, i.e.,

$$\tilde{P}_2(s, v_i R) = \frac{s^2}{s^2 + (v_i R)^2}. \tag{3.12}$$

Both forms will be used in the next section. Note that v_i is expected to be of the order of the equivalent electron velocity v_e but not necessarily equal to it.

In atomic scattering calculations, a specific functional form of the electron density is usually assumed, and then its Fourier transform yields the form factor. In the present case this procedure can be inverted and the electron densities (or equivalently the scattering potentials) corresponding to the form factors in Eq. (3.9) and Eq. (3.10) can be obtained using an inverse Fourier transform. This is done in Appendix B, where it is shown that the form factor in Eq. (3.9) corresponds to the time-honored exponentially screened Coulomb potential, while the one in Eq. (3.10) is related to a hydrogenic electron density, i.e., a $1/r$ potential changing to an exponentially-screened Coulomb potential at large distances from the origin.

IV. ANALYTICAL CALCULATIONS

When the form factors $\tilde{f}_s$ or $\tilde{f}_r$, and the ionization probability functions $\tilde{P}_1$ or $\tilde{P}_2$ are substituted in Eq. (3.8) the resulting cross sections can be calculated analytically. Some simplification and also some insight into the relative importance of various factors can be obtained using the substitution: $u = 1/s^2$. Introducing the notation

$$\alpha = \frac{1}{(2vR)^2}, \qquad \beta = \frac{1}{(v_i R)^2}, \qquad \kappa = \frac{4\pi Z^2 R^2}{v^2},$$
$$g(u) = \tilde{f}(s)|_{s^2=u^{-1}}, \qquad p(u,\beta) = \tilde{P}(s, v_i R)|_{s^2=u^{-1}}, \tag{4.1}$$

yields for the electron loss cross section

$$\sigma = \kappa\int_\alpha^\infty [1-g(u)]^2 p(u,\beta)du\,. \tag{4.2}$$

Here the whole cross-section dependence on the physical parameters of the collision is contained in the coefficient κ and the (energy- and target-dependent) parameters α and β.

Using the u representation, the approximated form factors for the singular and regular case respectively are written as

$$g_s(u) = \frac{u}{u+1}, \tag{4.3}$$

$$g_r(u) = \frac{u^2}{(u+\gamma)(u+\gamma^{-1})}, \tag{4.4}$$

while the target ionization probabilities are given by

$$p_1(u,\beta) = \begin{cases} 1 & \text{for } u \leq \beta \\ 0 & \text{for } u > \beta, \end{cases} \tag{4.5}$$

$$p_2(u,\beta) = \frac{\beta}{u+\beta}, \tag{4.6}$$

depending on whether a sharp cutoff or a gradual transition is assumed. The various combinations of these functions give rise to four different cross-section expressions, which are as follows.

Formulation s_1. Using g_s and p_1 in Eq. (4.2) yields

$$\sigma = \kappa \frac{\beta - \alpha}{(\alpha+1)(\beta+1)}. \tag{4.7}$$

Formulation s_2. Using g_s and p_2 in Eq. (4.2) yields

$$\sigma = \kappa \frac{\beta}{(\beta-1)^2}\left(\frac{\beta-1}{\alpha+1} - \ln\frac{\alpha+\beta}{\alpha+1}\right). \tag{4.8}$$

Formulation r_1. Using g_r and p_1 in Eq. (4.2) yields

$$\sigma = \kappa \frac{1}{(\gamma-\gamma^{-1})^2}\left[(\beta-\alpha)\left(\frac{\gamma^4}{(\alpha+\gamma)(\beta+\gamma)} + \frac{\gamma^{-4}}{(\alpha+\gamma^{-1})(\beta+\gamma^{-1})}\right) - \frac{2}{\gamma-\gamma^{-1}}\ln\frac{(\alpha+\gamma)(\beta+\gamma^{-1})}{(\beta+\gamma)(\alpha+\gamma^{-1})}\right]. \tag{4.9}$$

Formulation r_2. Using g_r and p_2 in (4.2) yields

$$\sigma = \kappa \frac{\beta}{(\gamma-\gamma^{-1})^2(\beta-\gamma)^2(\beta-\gamma^{-1})^2} \times\left[\frac{\gamma^4(\beta-\gamma)(\beta-\gamma^{-1})^2}{\alpha+\gamma} + \frac{\gamma^{-4}(\beta-\gamma^{-1})(\beta-\gamma)^2}{\alpha+\gamma^{-1}} - \left(\gamma^4 - 2\frac{\beta-\gamma}{\gamma-\gamma^{-1}}\right)(\beta-\gamma^{-1})^2\ln\frac{\alpha+\beta}{\alpha+\gamma} - \left(\gamma^{-4} + 2\frac{\beta-\gamma^{-1}}{\gamma-\gamma^{-1}}\right)(\beta-\gamma)^2\ln\frac{\alpha+\beta}{\alpha+\gamma^{-1}}\right]. \tag{4.10}$$

Note the difference in complexity between the results of the singular and regular formulations.

Before proceeding, one should notice that the formalism described above is incomplete. The $\tilde{f}(q)$ expressed in Eq. (3.2) is just the elastic part of the atomic form factor.[11] The omission of the inelastic part is not expected to change significantly the functional dependence of the calculated cross sections on the collision energy (except, possibly, at the low-energy end). However, there is quite probably an additional target Z dependence, beyond that which is included in the simple formulation presented here. In principle it should be possible to estimate explicitly the contribution of inelastic processes, using a formalism similar to the one described above. This was not done here because the complexity of the resulting expressions would be increased enormously. Instead, since one of the declared goals of this work was simplicity, it was assumed that the inelastic contribution can be approximated by multiplying the results of Eqs. (4.7)–(4.10) by a Z-dependent multiplier Q.

Traditionally, when using the Born approximation, the cross sections are presented as a product of an energy-dependent factor, and of the asymptotic collision-strength parameters I. These parameters can also be obtained from Eq. (4.2). However, in the present formulation the intimate connection between the I's and the electronic wave functions of the colliding atoms is lost, so that the value of this result is somewhat dubious. Nevertheless, for completeness sake, the detailed procedure and calculated results are shown in Appendix C.

V. RESULTS AND DISCUSSION

The four formulations s_1, s_2, r_1, and r_2 for the electron-loss cross section, given in Eqs. (4.7)–(4.10), contain three unknown quantities, namely v_i, R, and γ. As noted above, the inelastic correction adds a fourth unknown Q. The first unknown, v_i, is a property of the projectile alone, while the other three are expected to be target dependent.

Based on existing simplified atomic models the target dependence of R is expected to be of the form $R = R_0 Z^{C_R}$. For the sake of simplicity it is assumed that also γ and Q can be approximated by similar expressions, i.e., $\gamma = \gamma_0 Z^{C_\gamma}$ and $Q = Q_0 Z^{C_Q}$, respectively. With these substitutions, the electron-loss cross sections include seven (five in the case of the singular formulation) target-independent parameters. As noted above, the intent here is to predict cross sections for all possible targets over a broad range of energies. Therefore, having five (or even seven) adjustable parameters is not excessive.

The values of the parameters were obtained by fitting the cross section expressions in Eqs. (4.7)–(4.10) (multiplied by Q) to existing experimental values of electron-loss cross sections for H^0 and H^- colliding with He, Ne, Ar, and Xe targets. Figures 1 and 2 show the data, which span the energy range from 2 keV to 14 MeV. The data[12–23] are from a JAERI compilation,[12] except for two newer data sets[22,23] in the 1–7 MeV energy range. The fitting was done using the MINUIT optimization routine.[24]

The $\sigma_{0,1}$ results for each of the four different formulations mentioned above are shown in Figs. 3(a)–3(d). The left (right) half shows results for a gradual (sharp) ionization cutoff, while the top (bottom) half displays results for the singular (regular) formulation. The figure shows that reasonable fits were obtained in all cases, over a very broad energy range, and for all the targets used (range of Z from 2 to 54). The only possible prob-

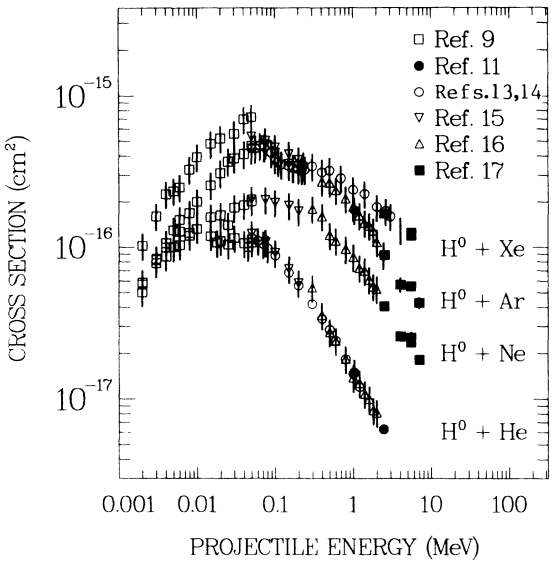

FIG. 1. Single-electron-loss cross-section data for H^0 colliding with He, Ne, Ar, and Xe.

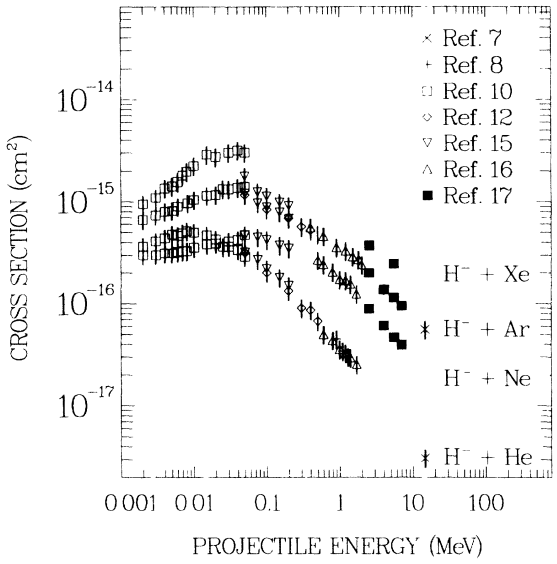

FIG. 2. Single-electron-loss cross-section data for H^- colliding with He, Ne, Ar, and Xe.

lem areas are low-energy (< 50 keV) results for Ar and Xe targets. However, Fig. 1 illustrates that experimental results from various laboratories differ by considerably more than their reported uncertainties. This clearly indicates that at least part of the low-energy data is not reliable. Therefore, until new and consistent data for low-energy electron-loss cross sections will become available, it is difficult to judge the quality of the fit for high-Z targets at the low-energy end. Still, in general, the FCM cross sections seem to reproduce the existing data down to significantly lower energies than could be expected given the free-collision assumption inherent in the model.

Comparison of the left half [(a) and (b)] and the right half [(c) and (d)] of Fig. 3 shows that the low-energy behavior is reproduced better using the gradual, rather than sharp, cutoff formulations. Given the fact that collisional ionization is known to occur at collision velocities well below Bohr velocity, this result was expected. Note that at high enough energies all four formulations yield virtually identical results regardless of the particular form of ionization probability used.

Comparison of the top half [(a) and (c)] and the bottom half [(b) and (d)] of Fig. 3 reveals that there is practically no difference between the quality of fits obtained using a regular electron density, as opposed to one with a singularity at the origin. This can be explained by noting that the form factors for singular and regular formulations differ only in the region of very large momentum transfers. This region is accessible only at very high collision velocities, and even then its contribution to the total cross section is limited. Moreover, since the cross section depends on the form factor only through the combination $1-\tilde{f}(s)$ [see Eq. (3.8)], even this small contribution is (to first order) independent of the form factor. In other words, the assumed (integrable) singularity of the electron distribution influences the result only through a modification of the screening in the immediate vicinity of the origin, where (as is well known) the screening is negligible anyway.

It could still be argued on pure theoretical grounds that the regular formulations are preferable to the (apparently nonphysical) singular ones. However, for practical applications the singular ones are preferable, because the results are similar, while the expressions obtained are much simpler. Since the results presented here are no longer strictly based on first principles, a localized violation of physical reality in a largely inaccessible region is a small price to pay for the resultant simplicity.

The $\sigma_{-1,0}$ results are shown in Figs. 4(a)–4(d). The data are from Fig. 2, where the disparity in results from different laboratories is even greater than for the $\sigma_{0,1}$ data of Fig. 1. The qualitative comparison of fits is similar to the $\sigma_{0,1}$ case, and all of the above observations apply. One could argue, of course, that the FCM based approach developed above is strictly a single-electron formalism, and that applying it to a two-electron ion like H^- is not justified. However, empirical evidence shows that (except possibly for extremely low collision velocities) $\sigma_{-1,0}$ scales with energy and target Z in the same way that $\sigma_{0,1}$ does. Therefore, it is not unreasonable to expect the same formalism to fit both processes.

VI. RECIPE FOR ESTIMATING ELECTRON-LOSS CROSS SECTIONS

The values of the parameters obtained by fitting the formulas in Eqs. (4.7)–(4.10) to the existing experimental H^0 and H^- data for $\sigma_{0,1}$ and $\sigma_{-1,0}$ are presented in

TABLE I. The parameters used to calculate $\sigma_{0,1}$.

	Formulation			
Parameter	s_1	s_2	r_1	r_2
v_i	0.50	0.70	0.50	0.70
R_0	0.34	0.40	0.11	0.11
C_R	-0.53	-0.54	-0.73	-0.73
Q_0	7.39	5.85	7.30	5.81
C_Q	0.35	0.29	0.35	0.29
γ_0			10.1	14.0
C_γ			0.39	0.38

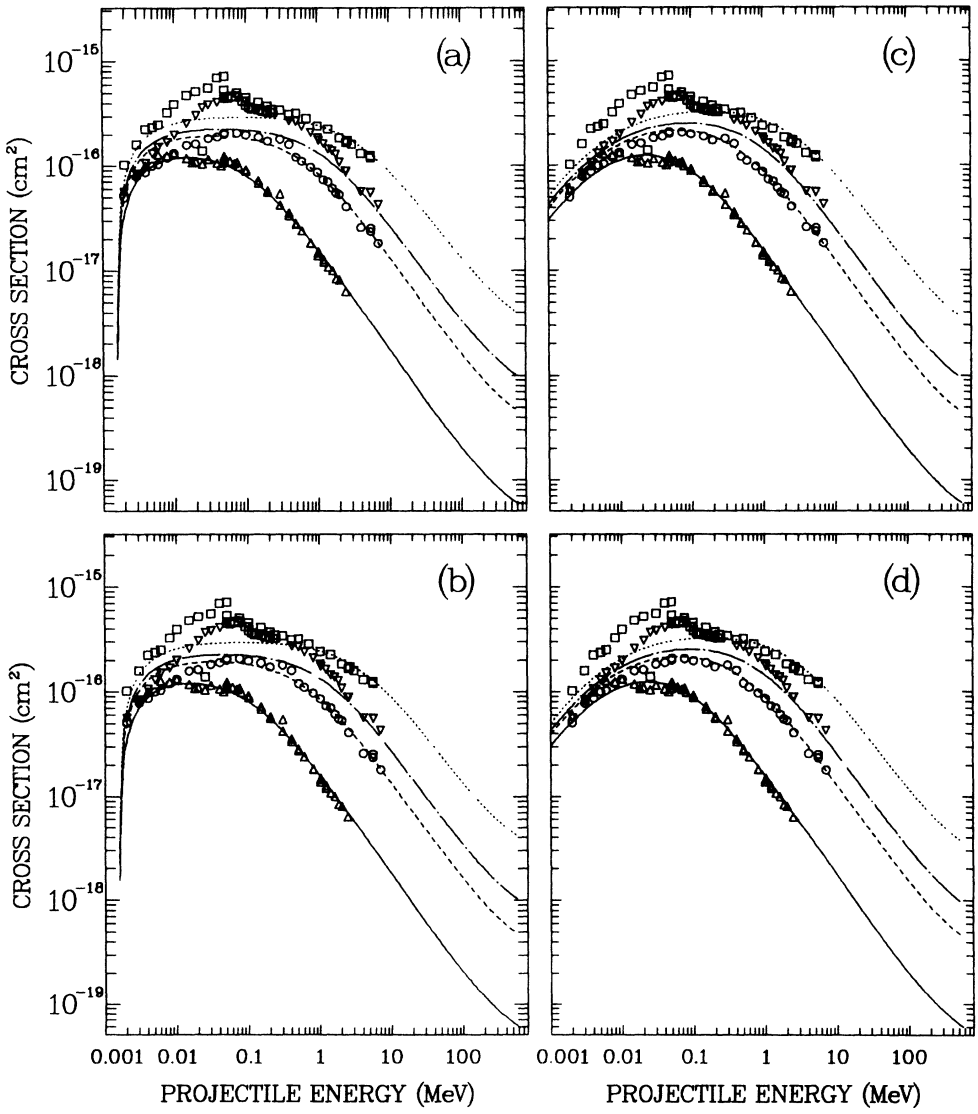

FIG. 3. Results obtained from fitting the four formulations (a) s_1, (b) r_1, (c) s_2, and (d) r_2 to the $\sigma_{0,1}$ data from Fig. 1. Here the symbols and curves refer to H^0 + He (△, solid line), H^0 + Ne (○, dashed line), H^0 + Ar (▽, dash-dotted line), and H^0 + Xe (□, dotted line).

TABLE II. The parameters used to calculate $\sigma_{-1,0}$.

	Formulation			
Parameter	s_1	s_2	r_1	r_2
v_i	0.35	0.28	0.33	0.25
R_0	0.26	0.26	0.24	0.23
C_R	-0.34	-0.34	-1.03	-0.95
Q_0	41.6	39.2	34.8	32.4
C_Q	-0.25	-0.26	-0.18	-0.18
γ_0			1.22	1.43
C_γ			1.37	1.20

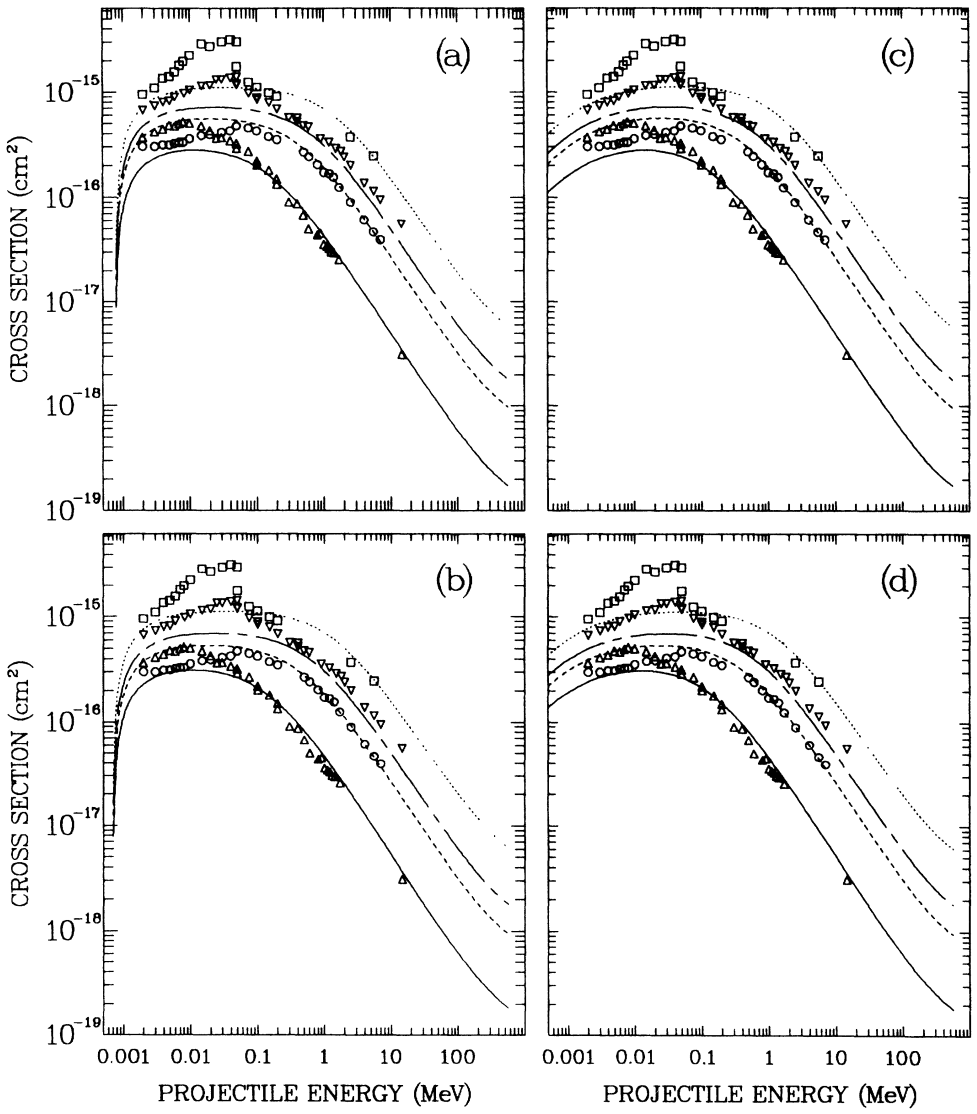

FIG. 4. Results obtained from fitting the four formulations (a) s_1, (b) r_1, (c) s_2, and (d) r_2 to the $\sigma_{-1,0}$ data from Fig. 2. Here the symbols and curves refer to H^0 + He (△, solid line), H^0 + Ne (○, dashed line), H^0 + Ar (▽, dash-dotted line), and H^0 + Xe (□, dotted line).

Tables I and II, respectively. Altogether there are seven parameters, namely v_i, R_0, C_R, γ_0, C_γ, Q_0, and C_Q. As stated above, these parameters can be used to estimate electron-loss cross sections for H^0 and H^-, for any target and virtually any collision energy.

The calculation is done as follows.

(1) The scaling radius R is obtained using the parameters R_0 and C_R, and the relation $R = R_0 Z^{C_R}$, where Z is the target atomic number.

(2) The values of α,β, and κ are obtained using R, v_i, the collision velocity v (in atomic units), and the substitutions in Eq. (4.1).

(3) If one of the regular formulations is used, γ is obtained using $\gamma = \gamma_0 Z^{C_\gamma}$.

(4) The values of κ, α, β, and, if needed, γ are used in one of the equations (4.7)–(4.10), depending on the formulation chosen.

(5) The cross section (in atomic units) is obtained by multiplying the result of the previous step by the appropriate value of Q, given by $Q = Q_0 Z^{C_Q}$.

Based on the previous discussion there seems to be no advantage in using one of the regular (as opposed to singular) formulations, while the amount of calculational effort is increased appreciably. It was also seen that the gradual (rather than sharp) cutoff formulations are preferable. Therefore the best combination of overall accuracy and ease of use is obtained using formulation s_2 [Eq. (4.8)].

VII. CONCLUSIONS

Analytical expressions for the electron-loss cross sections of hydrogenic ions were obtained using the FCM and simple estimates for target atomic form factors. Using only a few target-independent parameters a good fit has been obtained to the existing experimental data for He, Ne, Ar, and Xe, over an enormous energy range. Obviously the model can be extended to other projectiles, and possibly, with some modifications, to all the atomic processes in which the cross section can be expressed in terms of the form factors of the interacting atoms.

It may be that some of the assumptions used in the present work are too naive. Furthermore, the accuracy of the model might be further enhanced by using more detailed form-factor approximants. However, simplicity and ease of use should be balanced against precision, and new complicating factors should be introduced only when the benefits of doing so can be clearly demonstrated. Further development of this model must await a more extensive and more reliable set of experimental results. Experimentalists should strive to make low-uncertainty measurements over the widest possible range of collision velocities and target atomic number.

ACKNOWLEDGMENTS

This work was supported by the Fundamental Interactions Branch, Division of Chemical Sciences, Office of Basic Energy Sciences, U.S. Department of Energy, under Contract No. DE-AC02-76CH00016.

APPENDIX A: SIMPLE APPROXIMATIONS TO REDUCED FORM FACTORS

From Eq. (3.7) the reduced form factor $\tilde{f}(s)$ is given by

$$\tilde{f}(s) = \int_0^\infty t\tilde{\rho}(t)\frac{\sin st}{s}dt, \tag{A1}$$

where $\tilde{\rho}$ fulfills

$$\int_0^\infty t^2\tilde{\rho}(t)dt = 1. \tag{A2}$$

The form of Eq. (A1) implies that $\tilde{f}$ is an even function of s, and that it can have no poles for real values of s. Moreover, the asymptotic properties of $\tilde{f}$ for small and large values of s can be deduced from Eq. (A1) regardless of the exact functional shape of $\tilde{\rho}$.

For $s \ll 1$ a Taylor series development of the integrand in Eq. (A1) yields

$$\begin{aligned}\tilde{f}(s) &\approx \int_0^\infty t\tilde{\rho}(t)\left(t - \frac{t^3 s^2}{6}\right)dt \\ &= 1 - \frac{s^2}{6}\langle t^2\rangle \\ &= 1 - O(s^2).\end{aligned} \tag{A3}$$

For $s \gg 1$, an asymptotic series representation of $\tilde{f}$ can be obtained from Eq. (A1) using integration by parts. The first few terms of the series are

$$\tilde{f}(s) \approx \frac{1}{s^2}t\tilde{\rho}(t)\Big|_{t=0} - \frac{1}{s^4}[t\tilde{\rho}(t)]''\Big|_{t=0} + \cdots. \tag{A4}$$

Therefore, if $\tilde{\rho}$ is regular at the origin, then $\tilde{f}$ behaves asymptotically like $1/s^4$. This result is well known.[25,26] On the other hand, if $\tilde{\rho}$ has a $1/t$ singularity at the origin [which is allowable because the integral in Eq. (A2) will still converge], then $\tilde{f}$ is of the order of $1/s^2$ for large values of s. While not corresponding to a real physical situation, this result is nevertheless useful. The reasons for this are explained in Secs. III and V.

The simplest possible function whose small s behavior follows Eq. (A3) and whose asymptotic large s behavior corresponds to the singular case of Eq. (A4), is given by

$$\tilde{f}(s) = \frac{a^2}{s^2 + a^2}, \tag{A5}$$

where a is an arbitrary constant. If a singular $\tilde{\rho}$ is not acceptable, then the simplest function will be

$$\tilde{f}(s) = \frac{a^2 b^2}{(s^2 + a^2)(s^2 + b^2)}, \tag{A6}$$

where now the function contains two parameters, b and

c. It should be noted, however, that R in Eq. (3.6) is defined only to within a multiplicative constant, and the same is true for $s = qR$. This freedom can be used to further simplify the expressions in Eqs. (A5) and (A6). By properly choosing the constants the result for the singular formulation is

$$\tilde{f}(s) = \frac{1}{s^2+1}, \tag{A7}$$

and the result for the regular formulation is

$$\tilde{f}(s) = \frac{1}{(s^2+\gamma)(s^2+\gamma^{-1})}, \tag{A8}$$

where γ is an arbitrary constant, yet to be determined.

APPENDIX B: FORM-FACTOR INVERSION

From Eq. (3.7) the reduced form factor $\tilde{f}(s)$ is given by

$$\tilde{f}(s) = \int_0^\infty t\tilde{\rho}(t)\frac{\sin st}{s}dt. \tag{B1}$$

Applying an inverse Fourier transform and using the fact that both $\tilde{\rho}$ and $\tilde{f}$ are spherically symmetric, yields

$$\tilde{\rho}(t) = \frac{2}{\pi}\int_0^\infty s\tilde{f}(s)\frac{\sin st}{t}ds. \tag{B2}$$

Using also the fact that $\tilde{f}(s)$ is an even function of s allows to express the reduced electron density $\tilde{\rho}$ as

$$\tilde{\rho}(t) = \frac{1}{\pi i t}\int_{-\infty}^\infty s\tilde{f}(s)e^{ist}ds, \tag{B3}$$

which, evaluated using contour integration, yields

$$\tilde{\rho}(t) = \frac{2}{t}\sum_{up}\text{Res}\left[s\tilde{f}(s)e^{ist}\right], \tag{B4}$$

where the sum is over the residua in the upper half plane. Now, as the radial electron density is assumed to be of the form [see Eq. (3.6), text]

$$\rho(r) = \frac{1}{R^3}\tilde{\rho}\left(\frac{r}{R}\right), \tag{B5}$$

the final result for $\rho(r)$ is

$$\tilde{\rho}(r) = \frac{2}{R^2 r}\sum_{up}\text{Res}\left[s\tilde{f}(s)e^{is(r/R)}\right]. \tag{B6}$$

The electrostatic potential for a spherically symmetric charge density is given by

$$\begin{aligned}\Psi(\bar{r}) &= 4\pi\int_r^\infty \frac{dr'}{r'^2}\int_0^{r'} r''^2\rho(\bar{r}'')dr'' \\ &= \frac{4\pi}{r}\left(\int_0^\infty r'^2\rho(\bar{r}')dr' - \int_r^\infty r'(r'-r)\rho(\bar{r}')dr'\right),\end{aligned} \tag{B7}$$

where $\rho(\bar{r})$ is the full, three-dimensional charge density. In the spherically symmetric atomic case $\rho(\bar{r})$ can be written as

$$\rho(\bar{r}) = \frac{Z}{4\pi}\left(\frac{\delta(r)}{r^2} - \rho(r)\right), \tag{B8}$$

where $\rho(r)$ is the electron radial density. Substitution of Eq. (B8) into Eq. (B7) yields

$$\Psi(r) = \frac{Z}{r}\int_r^\infty r'(r'-r)\rho(r')dr'. \tag{B9}$$

Now, using again the scaling assumption $\rho(r) = (1/R^3)\tilde{\rho}(r/R)$, and the notation $t = r/R$, $\Psi(r)$ can be rewritten as

$$\Psi(r) = \frac{Z}{r}\int_t^\infty t'(t'-t)\tilde{\rho}(t')dt'. \tag{B10}$$

Substitution of the density $\tilde{\rho}(t)$ from Eq. (B3) into Eq. (B10) yields

$$\Psi(r) = \frac{Z}{\pi i r}\int_t^\infty (t'-t)dt'\int_{-\infty}^\infty s\tilde{f}(s)e^{ist'}ds. \tag{B11}$$

Using the additional substitution $u = t' - t$ and changing the order of integration we get

$$\Psi(r) = \frac{Z}{\pi i r}\int_{-\infty}^\infty s\tilde{f}(s)e^{ist}ds\int_0^\infty ue^{isu}du, \tag{B12}$$

which, using the well-known result

$$\int_0^\infty ue^{isu}du = \lim_{\epsilon\to+0}\frac{1}{(is-\epsilon)^2} = -\frac{1}{s^2}, \tag{B13}$$

can be converted into

$$\Psi(r) = -\frac{Z}{\pi i r}\int_{-\infty}^\infty \frac{1}{s}\tilde{f}(s)e^{ist}ds. \tag{B14}$$

Evaluation of this expression using contour integration over the complex upper half plane yields finally

$$\begin{aligned}\Psi(r) &= -\frac{2Z}{r}\sum_{up}\text{Res}\left(\frac{1}{s}\tilde{f}(s)e^{ist}\right) \\ &= -\frac{2Z}{r}\sum_{up}\text{Res}\left(\frac{1}{s}\tilde{f}(s)e^{isr/R}\right),\end{aligned} \tag{B15}$$

where again only the residua in the upper half plane are counted. Specifically the pole at $s = 0$ is excluded, being the limit of a pole in the lower half plane.

The results (B4) and (B15) can be applied to the reduced form factors $f_s(s)$ and $f_r(s)$ which were introduced in the text. For $f_s(s)$ the results are

$$\rho(r) = \frac{1}{R^2 r}e^{-r/R}, \tag{B16}$$

$$\Psi(r) = \frac{Z}{r}e^{-r/R}, \tag{B17}$$

i.e., the well-known exponentially screened Coulomb potential. For $f_r(s)$ on the other hand we get

$$\rho(r) = \frac{1}{R^2 r}\frac{e^{-\gamma^{-1/2}r/R} - e^{-\gamma^{1/2}r/R}}{\gamma - \gamma^{-1}}, \tag{B18}$$

$$\Psi(r) = \frac{Z}{r}\gamma\frac{e^{-\gamma^{-1/2}r/R} - \gamma^{-1}e^{-\gamma^{1/2}r/R}}{\gamma - \gamma^{-1}}, \tag{B19}$$

which, while being similar to the previous result at very large values of r, yields a finite electron density at $r = 0$. The divergence for $\gamma = 1$ is only apparent. Actually the limits of (B18) and (B19) for $\gamma = 1$ can be easily evaluated and the results are

$$\rho(r) = \frac{1}{2R^3} e^{-r/R}, \tag{B20}$$

$$\Psi(r) = \frac{Z}{r} e^{-r/R} \left(1 + \frac{r}{2R}\right). \tag{B21}$$

Apart from the scaling radius R these results are identical to the ones obtained using a hydrogenlike 1s wave function.

APPENDIX C: ASYMPTOTIC COLLISION STRENGTH PARAMETERS

The asymptotic collision strength I is formally given by

$$I = \lim_{v \to \infty} \frac{v^2}{8\pi} \sigma, \tag{C1}$$

which, using the cross section from Eq. (4.2), text, yields

$$I = \frac{Z^2 R^2}{2} \int_0^\infty [1 - g(u)]^2 P(u, \beta) du. \tag{C2}$$

Specific results for the four cases discussed in the text are for s_1,

$$I = \frac{Z^2 R^2}{2} \frac{\beta}{\beta + 1}; \tag{C3}$$

for s_2,

$$I = \frac{Z^2 R^2}{2} \frac{\beta(\beta - 1 - \ln \beta)}{(\beta - 1)^2}; \tag{C4}$$

for r_1,

$$I = \frac{Z^2 R^2}{2} \frac{1}{(\gamma - \gamma^{-1})^2} \left[\beta \left(\frac{\gamma^3}{\beta + \gamma} + \frac{\gamma^{-3}}{\beta + \gamma^{-1}} \right) - \frac{2}{\gamma - \gamma^{-1}} \ln \frac{\gamma(\beta + \gamma^{-1})}{\gamma^{-1}(\beta + \gamma)} \right]; \tag{C5}$$

and for r_2,

$$I = \frac{Z^2 R^2}{2} \frac{\beta}{(\gamma - \gamma^{-1})^2 (\beta - \gamma)^2 (\beta - \gamma^{-1})^2} \times \left[(\beta - \gamma)(\beta - \gamma^{-1}) \left[\gamma^3 (\beta - \gamma^{-1}) + \gamma^{-3} (\beta - \gamma) \right] - \left(\gamma^4 - 2 \frac{\beta - \gamma}{\gamma - \gamma^{-1}} \right) (\beta - \gamma^{-1})^2 \ln \beta \gamma^{-1} - \left(\gamma^{-4} + 2 \frac{\beta - \gamma^{-1}}{\gamma - \gamma^{-1}} \right) (\beta - \gamma)^2 \ln \beta \gamma \right]. \tag{C6}$$

Of course, all the results above need to be multiplied by the inelastic correction factor Q (see Sec. IV, bottom).

[1] G.H. Gillespie, Phys. Rev. A **16**, 943 (1977).
[2] G.H. Gillespie, Phys. Rev. A **18**, 1967 (1978).
[3] G.H. Gillespie and M. Inokuti, Phys. Rev. A **22**, 2430 (1980).
[4] D.P. Dewangan and H.R.J. Walters, J. Phys. B **11**, 3983 (1978).
[5] C. Taward *et al.*, J. Chim. Phys. **64**, 540 (1967).
[6] J. H. Hubbell *et al.*, J. Phys. Chem. Ref. Data **4**, 471 (1975).
[7] G. C. Lie, J. Phys. Soc. Jpn. **42**, 1327 (1977).
[8] Y. -K. Kim and M. Inokuti, Phys. Rev. **165**, 39 (1968).
[9] M. Naon and M. Cornille, J. Phys. B **5**, 1965 (1972).
[10] M. Naon, M. Cornille, and Y. -K. Kim, J. Phys. B **8**, 864 (1975).
[11] H.R.J. Walters (private communication).
[12] Y. Nakai, A. Kikuchi, T. Shirai, and M. Sataka, Japan Atomic Energy Research Institute Report No. JAERI-M 83-143, 1983 (unpublished), p. 66.
[13] R. Smythe and J.W. Toevs, Phys. Rev. **139**, A15 (1965).
[14] G.I. Dimov and V.G. Dudnikov, Zh. Tekh. Fiz **36**, 1239 (1967) [Sov. Phys. — Tech. Phys. **11**, 919 (1967)].
[15] J.F. Williams, Phys. Rev. **153**, 116 (1967).
[16] J.F. Williams, Phys. Rev. **154**, 9 (1967).
[17] L.M. Welsh, K.H. Berkner, S.N. Kaplan, and R.V. Pyle, Phys. Rev. **158**, 85 (1967).
[18] J. Heinemeier, P. Hvelplund, and F.R. Simpson, J. Phys. B **9**, 2669 (1976).
[19] E.H. Pedersen, L. Larsen, and J. Mikkelsen, J. Phys. B **10**, L669 (1977).
[20] E.H. Pedersen and L. Larsen, J. Phys. B **12**, 4099 (1979).
[21] C.J. Anderson, R.J.Girnius, A.M. Howald, and L.W. Anderson, Phys. Rev. A **22**, 822 (1980).
[22] D.P. Almeida, N.V. de Castro Faria, F.L. Freire, Jr., E.C. Montenegro, and A.G. de Pinho, Phys. Rev. A **36**, 16 (1987).
[23] M.Meron, B.M. Johnson and K.W.Jones, in Abstracts of Contributed Papers, XVI International Conference on the Physics of Electronic and Atomic Collisions, New York, 1989 (unpublished), p. 465; B.M. Johnson, M. Meron, D. Maor, and K.W. Jones (unpublished).
[24] Program Library, Division DD, CERN, CH-1211 Geneva 23, Switzerland.
[25] V. H. Smith, Chem. Phys. Lett. **7**, 226 (1970).
[26] O. Goscinski and P. Lindner, J. Chem. Phys. **52**, 2539 (1970).